Inorg. Chem. **2004**, *43*, 3371–3376

Synthesis, Structure, and Bonding of $Lu_7Z_2Te_2$ (Z = Ni, Pd, Ru). Linking Typical Tricapped Trigonal Prisms in Metal-Rich Compounds

Ling Chen and John D. Corbett*

Department of Chemistry, Iowa State University, Ames, Iowa 50011

Received August 22, 2003

The syntheses and structures of and bonding in the title compounds are described and compared with those for the isostructural orthorhombic $Er_7Ni_2Te_2$ (*Imm*2) and other related phases. Single-crystal data are reported for Z = Ni, Pd. The condensation of tricapped trigonal prisms (TTP) into sheets and the bridging of these by separate Lu atoms into a 3D structure are described. The interlayer separation, the Lu–Lu bonding achieved, and the polar Lu–Te bonding therewith are all affected by the size and valence energies of Te. The two Te spacers also exist in capped centered Lu_6Te trigonal prisms. In terms of extended Hückel band analyses, the overall bonding for both Lu–Ni and Lu–Te are optimized energetically, but not for Lu–Lu. The average Lu–Lu overlap populations about each Lu appropriately increase with a decrease in the number of its Te neighbors.

Introduction

The term "metal-rich compounds" normally refers to those having metal-to-nonmetal ratios greater than one. These usually exhibit metal−metal bonding in diverse motifs such as isolated metal clusters, 1D metal chains, 2D sheets, or 3D networks when nonmetal atoms are also present. To some extent, the additional incorporation of late transition metals into earlier transition metal frameworks allows one access to a growing and diverse field of new ternary phases, particularly for metal-rich chalcogenides. The extra stability of such polar heteroatomic metal−metal interactions was evidently first noted by Brewer and Wengert[1] in terms of Lewis acid−base interactions between electron-poor early transition metals and the electron-rich late transition metals. The chalcogenides are in a very general way comparable to the interstitially-stabilized reduced metal halides, with the additional central bonding and bonding electrons afforded by the interstitial atoms, but with reduced dimensionality in the latter because of the greater proportion of anions in the halides.[2] Of course, the salt-like nature of such ternary phases also makes major contributions to the overall stability of the whole structures in terms of their Coulombic (Madelung) energies.

Customarily, the late transition metal atoms center polyhedra of the early transition metals. To date, there are nine different formula types for such ternary metal-rich chalcogenides in terms of the proportions of early transition metal to the later centered metal to chalcogen (M:Z:Ch). There appear to be three categories in terms of building units. The most common is the Z-centered tricapped trigonal prism (TTP) that occurs in the following order of increasing Z concentration: 8:1:8 (Ta_8NiSe_8[3]), 8:1:6 (Hf_8ZTe_6[4]), 11:2:8 ($Ta_{11}Z_2Se_8$[5]), 5:1:3 (Hf_5FeTe_3[6]), 6:1:2 (M_6ZTe_2[7−10]), 9:2:6 ($Ta_9Z_2S_6$[11,12]), and 7:2:2 ($Er_7Ni_2Te_2$[13]). The ways of interlinking these Z-centered TTP in these are naturally different; the TTP aggregations appear to be influenced first by the ratio of host M to centered Z, and, second, by the *Ch* proportion as well. For example, the structures M_6ZTe_2[7−10] and Hf_5FeTe_3[6] contain 3D networks of single and double TTP-based chains, whereas the network in $Er_7Z_2Te_2$, Z = Ni, Co,[13] has TTP-based layers with a different kind of interlayer connection. It is interesting that numerous reduced transition metal halides show no examples with centered TTP units—rather the most common building unit is the centered octahedron. The higher proportion of nonmetal in the halide

* Author to whom correspondence should be addressed. E-mail: jcorbett@iastate.edu.

(1) Brewer, L.; Wengert, P. R. *Metallurg. Trans.* **1973**, *4*, 2674.
(2) Corbett, J. D. *Inorg. Chem.* **2000**, *39*, 5178.
(3) Conrad, M.; Harbrecht, B. *J. Alloys Compd.* **1993**, *197*, 57.
(4) Abdon, R. L.; Hughbanks, T. *Chem. Mater.* **1994**, *6*, 424.
(5) Harbrecht, B. *J. Less-Common Met.* **1988**, *144*, 59.
(6) Abdon, R. L.; Hughbanks, T. *J. Am. Chem. Soc.* **1995**, *117*, 10035.
(7) Wang, C.; Hughbanks, T. *Inorg. Chem.* **1996**, *35*, 6987.
(8) Maggard, P. A.; Corbett, J. D. *Inorg. Chem.* **2000**, *39*, 4143.
(9) Bestaoui, N.; Herle, P. S.; Corbett, J. D. *J. Solid State Chem.* **2000**, *155*, 9.
(10) Chen, L.; Corbett, J. D. *Inorg. Chem.* **2004**, *43*, 436.
(11) Harbrecht, B.; Franzen, H. F. *J. Less-Common Met.* **1985**, *113*, 349.
(12) Harbrecht, B. *J. Less-Common Met.* **1986**, *124*, 125.
(13) Meng, F. Q.; Hughbanks, T. *Inorg. Chem.* **2001**, *40*, 2482.

10.1021/ic030261k CCC: $27.50
Published on Web 05/07/2004

examples appears to be the principal factor, inasmuch as average number of electrons per metal atom may be very similar.[14]

The second category contains Z-centered square antiprisms as found in 4:1:4 (Ta_4ZTe_4[15]) (Z = Cr, Fe−Ni, Al, Si) and 14:3:8 ($Sc_{14}Z_3Te_8$[16]) (Z = Os, Ru). It is worth noting that the antiprismatic unit occurs in reduced halides as well and with about the same M:Z proportions, 4:1:4 (R_4OsBr_4[17]) and 4:1:2 (Ti_4ZBr_2, Z = Cr−Ni[18]) despite the differences in both electron counts per metal and the anions. Interchain bridging functions are very different in the two groups, though.

The third group involves Z-centered trigonal prisms that share rectangular faces (FTP). These compounds have higher Z proportions, and the centered atoms additionally bond to each other to form metal−metal chains, though sometimes a weakly bonded one, e.g., for 5:2:2 ($Sc_5Ni_2Te_2$,[19] vs $Y_5Ni_2Te_2$[20,21]). This motif is also found in one halide in which the concept of a centering atom has almost disappeared, for 2:2:1(Pr_2Ni_2I[22]).

The rare-earth elements R as the first group of transition metals have the fewest valence electrons in relatively large d orbitals, and this aspect appears to give a new chemistry in related metal−metal frameworks in chalcogenides, often over extremes among the R elements, viz., Lu_7Te and Lu_8Te[23] with unprecedented structures and Lu_7Sb_3[14] which is isostructural with Sc_7As_3.[24] Other rare-earth-metal compounds may also show some particular similarities to metal-rich compounds of the following transition metals, especially for the heavier R, viz., $Lu_{11}Te_4$[14] which is basically isostructural with $Ti_{11}Se_4$;[25] Sc_8Te_3 which appears to be clearly related to Ti_8S_3 but with fewer electrons and a much larger "spacer" nonmetal;[26] Sc_9Te_2 which is related to Ti_9Se_2;[20] and Sc_6FeTe_2 and others which are isotypic with a number of M_6ZNm phases, M = Zr, Hf, Nm = As, Sb, Te.[8] In this paper, we report the synthesis and structure of three isotypic orthorhombic compounds $Lu_7Z_2Te_2$ (Z = Ni, Pd, Ru) (*Imm*2), isostructural with $Er_7Ni_2Te_2$,[13] which represent other ways of linking typical TTP units, and we discuss their bonding characteristics as well as some further details about the structure type.

Experimental Section

Syntheses. All materials were handled in an Ar-filled glovebox to reduce contamination. The starting materials were Lu metal powder (Ames Lab 99.99% total), Ni, Pd, and Ru powders (Alfa, >99.5% metals basis), and Te ingots (Aldrich, 99.99%). No impurity in any of the starting materials was detected by energy-dispersive X-ray (EDX) analyses as well.

To reduce Te activities in subsequent reactions, Lu_2Te_3 (orthorhombic, Sc_2S_3 type) was synthesized after mixing Lu and Te in 2:3 proportions in a fused silica tube that was then sealed off in a high vacuum and heated to 450 °C for 12 h and then to 900 °C for 72 h. Guinier-X-ray powder diffraction data showed only the target phase. This was mixed with appropriate amounts of Lu metal and Ni, Pd, or Ru to give 7:2:2 atom ratios and then pelletized with the aid of a hydraulic press located within the glovebox. The mixture was arc-melted on a water-cooled copper hearth within the box with a 30 ampere current for 20 s per side; the weight loss with Ni, Pd, and Ru examples being 0.9, 0.5, and 0.6 wt %, respectively. The buttons were crushed into smaller pieces with the aid of an agate mortar, and then ground into fine black powders for powder diffraction analyses. The last showed high yields of the corresponding $Lu_7Z_2Te_2$ product for Ni and Pd (>95%) with no other phases observed, whereas unknown phases were observed as well with Ru.

The repelleted samples were wrapped in Mo foil, sealed into tantalum tubing, annealed in a graphite-heated high vacuum furnace with a residual pressure of less than 10^{-6} Torr at 1200 °C for 48 h, and then cooled to 800 °C at 10 °C/h. The pellets had usually partially melted, and small crystals from Ni, Pd, and Ru reactions that were suitable for single-crystal X-ray diffraction could be picked from the products or from the inner surface of the Mo foils. The powder diffraction data after annealing were for the most part similar to those obtained before, and the yields of the target compounds (according to relative intensities from the diffraction components) were ~90% except for the Ru target which was only 50% with 30% of an unknown. The only other observed impurity was LuTe (NaCl type). This last result suggests that small amounts of the products decomposed into LuTe and Ni or Pd and Lu metal during the 1200 °C annealing. Both Ni and Lu or their compounds attack the Mo foil somewhat as this became a little brittle during annealing, and Ni is known to diffuse into the outer Ta container at high temperatures.[8,9] Similar synthetic attempts with Os yielded only unknown products.

Powder X-ray Diffraction. The powder diffraction patterns of the $Lu_7Z_2Te_2$ phases were obtained with the aid of an Enraf-Nonius FR-552 Guinier powder camera and monochromatic Cu Kα1 radiation. The powdered samples mixed with internal standard Si (NIST) were each placed between two strips of cellophane tape on a frame that mounted on the sample rotation motor. Some powder patterns were also secured with the aid of a Huber G670 Guinier camera with an imaging plate. These powdered samples were held between Mylar films by a little petrolatum and in turn mounted on the sample holder. Data were collected over 15−60 min, depending on whether the needs were for identification or precision.

Single-Crystal Diffraction Studies. Several beautifully faceted black crystals of $Lu_7Ni_2Te_2$ were selected and sealed inside 0.3-mm i.d. thin-walled capillaries. Data collection was made with the aid of a Bruker APEX CCD-based X-ray diffractometer. A total of 1315 frames to $2\theta = 60°$ were collected with exposure times of 10 s per frame. The unit cell parameters listed in Table 1 were obtained from single-crystal data. The reflection intensities were integrated with the SAINT[27] subprogram, and absorption effects were corrected by SADABS.[28] The observation condition $h + k + l = 2n$ indicated a body-centered cell, and the mean value of

(14) Chen, L.; Corbett, J. D. unpublished work.
(15) Badding, M.; DiSalvo, F. J. *Inorg. Chem.* **1990**, *29*, 3952.
(16) Chen, L.; Corbett, J. D. *J. Am. Chem. Soc.* **2003**, *125*, 1170.
(17) Dorhout, P.; Corbett, J. D. *J. Am. Chem. Soc.* **1992**, *114*, 1697.
(18) Richter, C. G.; Jeitschko, W.; Künner, B.; Gerdes, M. *J. Solid State Chem.* **1997**, *137*, 400.
(19) Maggard, P. A.; Corbett, J. D. *Inorg. Chem.* **1999**, *38*, 1945.
(20) Maggard, P. A.; Corbett, J. D. *J. Am. Chem. Soc.* **2000**, *122*, 838, 10740.
(21) Maggard, P. A.; Corbett, J. D. *Inorg. Chem.* **2004**, *43*, 2556.
(22) Park, Y.; Martin, J. D.; Corbett, J. D. *J. Solid State Chem.* **1997**, *129*, 277.
(23) Chen, L.; Corbett, J. D. *J. Am. Chem. Soc.* **2003**, *125*, 7794.
(24) (a) Berger, R. *Acta Chem. Scand.* **1977**, *A31*, 514. (b) Berger, R.; Nolaeng, B. I.; Tergenius, L. E. *Acta Chem. Scand.* **1981**, *A35*, 679.
(25) Weirich, T. E.; Ramlau, R.; Simon, A.; Hovmöller, S.; Zou, X. *Nature* **1996**, *382*, 144.
(26) Maggard, P. A.; Corbett, J. D. *Inorg. Chem.* **1998**, *37*, 814.
(27) SAINT; Bruker AXS, Inc.: Madison, WI, 2000.
(28) Blessing, R. H. *Acta Crystallogr.* **1995**, *A51*, 33.

Table 1. Lattice Parameters (Å) and Cell Volumes ($Å^3$) of Orthorhombic $Lu_7Z_2Te_2$ Compounds[a]

Z	*a*	*b*	*c*	*V*
Ni	3.8169(6)	15.0863(3)	9.377(2)	539.9(2)
Pd	3.8841(8)	15.190(3)	9.448(2)	557.5(2)
Ru	3.817(1)	15.102(6)	9.375(3)	540.4(6)

[a] 992, 985, and 681 diffractometer peaks were indexed and refined on the APEX diffractometer for Ni, Pd, and Ru, respectively.

Table 2. Some Crystal and Refinement Parameters

	$Lu_7Ni_2Te_2$	$Lu_7Pd_2Te_2$
fw	1597.41	1692.79
cryst syst	orthorhombic	orthorhombic
space group, Z[a]	*Imm*2 (No. 44), 2	*Imm*2 (No. 44), 2
d_{calc} (g/cm^3)	9.826	10.085
μ (Mo Kα, mm^{-1})	71.958	69.546
R1, wR2 ($I > 2\sigma(I)$)[b]	0.0218, 0.0499	0.0267, 0.0480

[a] Unit cell parameters in Table 1. [b] $R1 = \sum||F_o| - |F_c||/\sum|F_o|$; $wR2 = [\sum w(|F_o|^2 - |F_c|^2)^2/\sum wF_o^2]^{1/2}$; $w^{-1} = [\sigma^2(F_o^2)]$ for $Lu_7Ni_2Te_2$; w^{-1} for $Lu_7Pd_2Te_2 = [\sigma^2(F_o^2) + (0.0070p)^2 + 1.00p]$ in which $p = (\mathrm{Max}(F_o^2, 0) + 2F_c^2)/3$.

$|E^2-1| = 0.643$ strongly suggested acentricity. Also, $R_{(int)} = 0.032$ meant that the Laue group *mmm* had been correctly assigned and appropriate equivalent reflections had been measured. The highest symmetry member of the three possible space groups, *Imm*2 (No. 44), was therefore chosen. The structure was solved by direct methods and refined with SHELXTL 6.10 [29] with one constraint on the origin. The anisotropic refinement converged to R1 = 0.0218, *w*R2 = 0.0499 for $I > 2\sigma(I)$ data. The Flack parameter = 0.01(2) indicated that the absolute structure was correct. The largest peak in the final ΔF map was 1.98 $e^-Å^{-3}$, 0.88 Å from Lu1, and the largest hole was -1.35 $e^-/Å^{-3}$, 1.49 Å from Lu1. The subsequent refinement of $Lu_7Pd_2Te_2$ was uneventful (R1 = 0.0267, wR2 = 0.0478 for all data).

Some data for these processes are listed in Table 2. The additional data collection and refinement parameters, the atomic positions, anisotropic displacement parameters, and a complete distance list are contained in the Supporting Information.

Band Calculations. The extended Hückel band calculations on $Lu_7Ni_2Te_2$ were carried out using the CAESAR program.[30] Because the states of the 3d metals in these compounds differ so greatly from those in normal situations,[31] the valence state ionization energies (H_{ii} values) of Ni and Te were taken from the iterated values derived for Sc_6NiTe_2.[8] Similarly, the H_{ii} values of Lu were obtained from Lu_8Te studies with the same Te data.[10] The parameters (eV) utilized for s, p, d for Lu and Ni were as follows: Lu -7.46, -4.62, -6.00; Ni -5.58, -4.21, -7.82, respectively; and for s, p of Te -21.20, -12.00 eV.

Results and Discussion

Structural Description. A near-[100] section of the orthorhombic $Lu_7Ni_2Te_2$ structure viewed along the short 3.82 Å *a* axis is given in Figure 1. The basic building units are distorted: Ni-centered trigonal prisms of Lu that share triangular (basal) faces with like units along the *a* axis to form infinite chains. These prismatic units are further

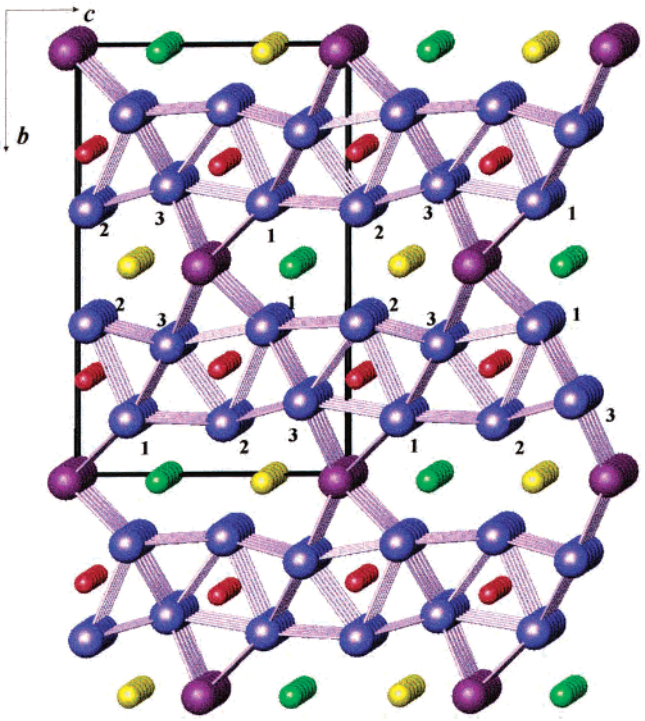

Figure 1. Off-[100] section of the orthorhombic $Lu_7Ni_2Te_2$ structure along the short *a* axis with the cell marked: red, Ni; purple, Lu1−3; magenta, Lu4; green, Te2; yellow, Te1. The Ni−Lu and Te−Lu contacts are not marked for clarity. All atoms lie on mirror planes at $x = 0, 1/2$.

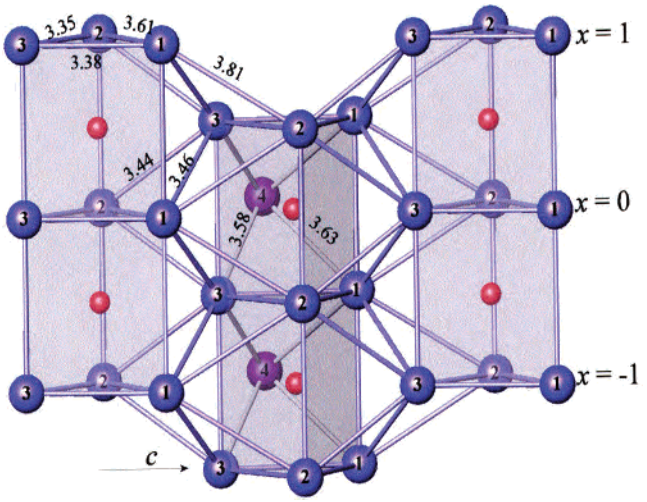

Figure 2. Ni-centered TTP relationships along *c* (right) and *a* (up): purple and magenta, Lu; red, Ni. Only the full TTP surroundings in the middle unit are shown for clarity. Ni−$Lu1_b$, 2.80 Å; Ni−$Lu1_c$, 3.63 Å; Ni−$Lu2_b$, 2.74 Å; Ni−$Lu3_b$, 2.74 Å; Ni−$Lu3_c$, 3.12 Å; Ni−$Lu4_c$, 3.62 Å.

interbonded in the *c* direction in a common manner in which two rectangular faces are capped by basal Lu atoms in two adjoining prismatic chains that are displaced by *a*/2. Then the third face-capping Lu4 atoms (magenta) bridge these to like neighboring units. The first process generates layers of trigonal prisms normal to $\vec{b}$, which are shown in Figure 2, and the second process interconnects these along $\vec{b}$ to give a 3D structure, Figure 1. From a larger viewpoint, the first step represents a widespread mode of condensation of tricapped trigonal prisms (TTP). But the lower symmetry environments in the present instance also lead to appreciable

(29) SHELXTL 6.10, Bruker AXS, Inc.: Madison, WI, 2000.
(30) Ren, J.; Liang, W.; Whangbo, M.-H. *CAESAR for Windows*; Prime-Color Software, Inc.; North Carolina State University: Raleigh, NC, 1998.
(31) Hughbanks, T.; Rosenthal, G.; Corbett, J. D. *J. Am. Chem. Soc.* **1988**, *110*, 1511.

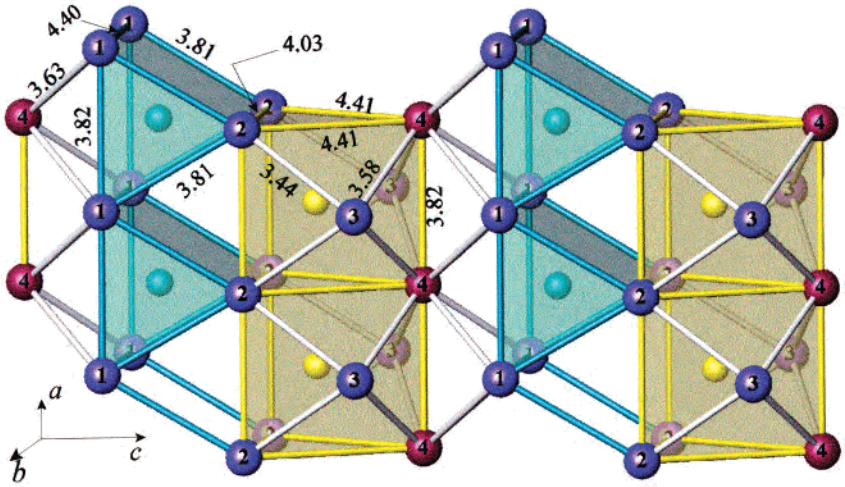

Figure 3. View slightly off [010] of the Te2 (green)- and Te1 (yellow)-centered polyhedra. Like pairs of atoms along *a* are 3.82 Å apart. Te2−Lu1, 3.08 Å (×4); Te2−Lu2, 3.05 Å (×2); Te2−Lu4$_c$, 3.18 Å; Te1−Lu2, 3.12 Å (× 4); Te1−Lu4, 3.14 Å (× 2); Te1−Lu3$_c$, 3.10 Å (×2).

distortions in distances, and some discussion is necessary. For example, the separations between face-capping Lu atoms and the centering Ni vary from 3.12 Å (Lu3) and ~3.62 Å (Lu1, Lu4) to ~2.76 Å for average Ni−Lu within the trigonal prisms. If Lu4, Lu3, and Lu1 are designated as *capping* atoms (*c*) and Lu1, Lu2, and Lu3 are designated as *basal* atoms (*b*), the basal bonds *d*(Lu$_b$−Lu$_b$) vary from 3.35 to 3.61 Å with an average of 3.45 Å, and the cap−base *d*(Lu$_c$−Lu$_b$) distances range over 3.44 to 3.81 Å, averaging only 3.8% longer than the first. (The longer prism edges between basal faces, attributable to the Te size, are not included in this analysis.) Although Lu2 serves only as a basal atom and Lu4 is just a capping atom, Lu1 and Lu3 atoms play dual roles, basal in one TTP and capping in another; see Figure 2. The lower symmetry and distortion in this structure are reflected in recognizable differences in distances by type. Although the number of Lu neighbors about the four Lu types at <4.0 Å range from 7 to 10, the respective distances about Lu1, Lu2, and Lu4 average nearly the same, 3.640−3.646 Å, which seems all the more unusual because of the different role of and environment about Lu4 (below). The eight distances about Lu3 average ~0.07 Å less (3.574 Å). The average Lu−Te distances about each Lu type span only a small range, 3.081 (Lu1) to 3.115 (Lu4), although the number of Te neighbors ranges from three (for Lu2 and Lu4) to one for Lu3. The last fact is probably the reason for shorter Lu−Lu distances about Lu3, as Te neighbors are known to detract from good bonding between the rare-earth metal atoms.[19−21] Moreover, the average Lu−Lu bonding separation in this structure, 3.63 Å, including prism edges, is appropriately longer than that in the metal-richer Lu_8Te, 3.43 Å, and Lu_7Te, 3.45 Å,[22] and shorter than that in the more oxidized Lu_6MoSb_2, 3.68 Å,[10] illustrating how oxidation by Te evidently drains electron density from the metallic network region onto the energetically lower-lying states of tellurium and thus weakens the overall Lu−Lu bonding. Still, it should be recognized that changes in coordination number and a relatively fixed R−Te tight packing also affect such comparisons.

In other comparisons, the average Ni−Lu$_b$ separation of 2.76 Å is comparable to 2.84 Å in LuNi[32] (FeB type) and 2.94 Å in intermetallic $LuNi_2$[33] (Cu_2Mg type), as well as in similar centered TTP compounds, viz., 2.81 Å in Dy_6FeTe_2.[9]

The structure becomes more diverse when we consider the region between the more or less regular trigonal prismatic layers of Figure 2 in which the two types of Te atoms along with the Lu4 atoms lie in the (020) planes of the structure. As shown in Figure 3, Te2 (green, CN6) centers a monocapped TP formed by Lu1,2 atoms, and Te1 (yellow, CN8) lies in a more regular bicapped TP bonding polyhedron, in contrast to the Ni centering of TP above. This feature means this structure type resembles some aspects of the Fe_2P-type structure as well, which is known for numerous combinations R_6MTe_2.[10] The combined arrangement is novel here in that the trigonal prisms (TP) around Te2 (green) face along $\vec{b}$ but do not share basal faces in that direction, rather only Lu1−Lu1 edges along $\vec{a}$ whereas the TP enclosing Te1 (yellow) form regular confacial chains along $\vec{a}$. The former are capped on one face by the bridging Lu4 whereas the chains enclosing Te1 include Lu4 and are externally capped by two Lu3 atoms (Figure 3). Note that the marked Lu−Lu distances within these last two TP are relatively large, ≥3.81 Å, compared with those about capping Lu3 and Lu4 that remain characteristically shorter, Table 3. In particular, the heights (side edges) of the green TP about Te2 and the basal edges around Te1 are over 4.00 Å and are not included in the quoted *d*(Lu−Lu) ranges and averages. The former direction lies vertical between the TP layers in Figure 1, along $\vec{b}$, which may be viewed as a result of both the complexity of the packing and the layer separation maintained by Lu4. But the average Te−Lu$_b$ distances, 3.07 Å around Te2, 3.1 Å about Te1, are similar to each other and to similar coordination polyhedra elsewhere, 3.13 Å in $Er_7Ni_2Te_2$[13] and 3.10 Å (CN6) in Lu_8Te,[23] but not to 3.24 Å,

(32) Dwight, A. E.; Conner, R. A.; Downey, J. W. *Acta Crystallogr.* **1965**, *18*, 837.
(33) Kripyakevich, P. I.; Teslyuk, M. Yu.; Frankevich, D. P. *Soviet Phys.-Crystallogr.* **1965**, *10* (3), 344.

Table 3. Selected Bond Distances (Å) and Mulliken Overlap Populations (MOP) in $Lu_7Ni_2Te_2$ by Bond Type

	bond	MOP
	trigonal base Lu_b-Lu_b[a]	
Lu1−Lu2 (1×)	3.61	0.275
Lu1−Lu3 (1×)	3.38	0.359
Lu3−Lu2 (1×)	3.35	0.335
	cap−base Lu_c-Lu_b[b]	
Lu1−Lu2 (2×)	3.81	0.150
Lu1−Lu3 (2×)	3.46	0.335
Lu3−Lu2 (2×)	3.44	0.250
	interlayer Lu_c-Lu_b	
Lu4−Lu1 (4×)	3.63	0.249
Lu4−Lu3 (4×)	3.58	0.256
	Ni−Lu[a]	
Ni−Lu_b (aver.)	2.76	0.280
Ni−$Lu3_c$ (1×)	3.13	0.176
Ni−$Lu4_c$ (1×)	3.62	0.085
Ni−$Lu4_c$ (1×)	3.63	0.088
	Te−Lu	
Te−Lu (aver.)	3.10	0.328
	pairwise along *a*	
Lu−Lu	3.82	0.180
Ni−Ni	3.82	−0.006
Te−Te	3.82	−0.03

[a] $_b$, base; $_c$, cap. [b] Interactions within layers normal to [010].

the sum of Shannon crystal radii (Lu^{3+}, Te^{2-}) for the CN6 and CN9 atoms, respectively.[34] All of these are longer than the 2.98 Å in LuTe (NaCl type).[35] It seems clear that the Lu−Te interactions in 7:2:2 phase are fairly strong and contribute considerably to the stability of the compound. The most unusual feature of Lu4 as an interlayer bonding feature that caps TP faces in two adjoining layers is that it has *no* Ni neighbors relative to the others, the nearest being over 0.8 Å farther away. The Mulliken overlap population (MOP) analyses from extended Hückel calculations are consistent with this circumstance (below).

The structure of the isostructural $Lu_7Pd_2Te_2$ (Supporting Information) does not reveal much beyond a general expansion of the lattice expected for the larger interstitial. The Lu−Lu distances by atom type increase modestly by 0.02 (Lu4) to 0.05 Å (Lu1), mostly along the TP heights. Likewise the Lu−Z distances increase by 0.05 to 0.07 Å, compared with 0.13 Å according to the difference in Pauling's single-bond metallic radii. There is only a 0.05 eV increase in Mulliken electronegativities associated with this change in Z.[36] Changes in Lu−Te distances are −0.010 Å to +0.007 Å (Lu4). Calculations were not pursued because of the generally rather uniform dimensional variations.

Theoretical Calculations. Electron band structure calculations for $Lu_7Ni_2Te_2$ were carried out within the extended Hückel tight binding method with the aid of the CAESAR[30] package. Figure 4 shows the total densities-of-states (DOS) and the partial DOS for the components on the left and Lu−Lu, Lu−Ni, Lu−Te crystal orbital overlap population (COOP) data on the right. The Fermi level intersects a prominent conduction band of mainly Lu 5d character, but

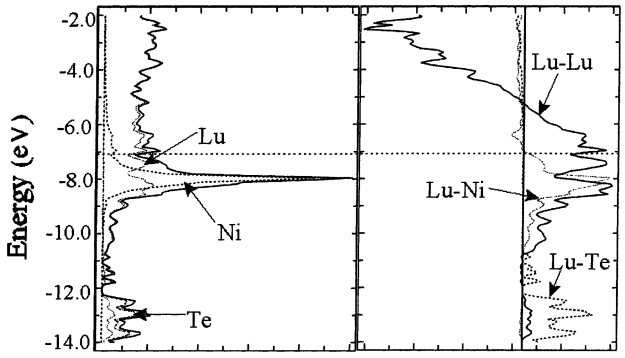

Figure 4. Total DOS (left) and COOP (right) data calculated for $Lu_7Ni_2Te_2$. The solid, dotted, dashed, and dash−dotted lines refer to total DOS and partial DOS of Lu, Ni, and Te, respectively. In the COOP plots, the solid, dotted, and dashed lines represent data for all Lu−Lu separations within 3.82 Å, all Lu−Ni contacts within 3.63 Å, and all Lu−Te interactions within 3.2 Å, respectively.

Table 4. Changes in Lu−Lu Bond Distances (Å) and MOP in $Lu_7Ni_2Te_2$ with Changes in Polar Bonding to Te and Ni, by Lu Atom Type

	Lu2	Lu4	Lu1	Lu3
CN	12	13	14	11
Ni, Te neighbors	2Ni 3Te	0Ni 3Te	2Ni 2Te	2Ni 1Te
average *d* (Lu−Lu) (Å)	3.610	3.646	3.643	3.574
average MOP (Lu−Lu)	0.235	0.251	0.263	0.297

comes just above the Ni core contributions mixed with Lu 5d. The data suggest (at this level) that this material is a metallic conductor, as expected from the structure and composition. Bands around −14.0 to −11.0 eV consist mainly of Te 5p and Lu 6s (and 5d) states that contribute to the Lu−Te polar bonding interactions. The reapportionment of the electron densities from the Lu−Lu metallic network into the energetically lower-lying states of Ni and Te helps stabilize the compound. The COOP data show that Lu−Ni and of course Lu−Te bonding are optimized in that all of the bonding states are filled, but considerable Lu−Lu interactions remain bonding above the Fermi level, characteristic of metal-rich and electron-poor compounds, as previously found for other examples.[16,19−21,23]

The strengths of the separate pairwise bonding interactions can be qualitatively related in terms of the COOP data (Figure 4, right) and, more quantitatively, in terms of the corresponding Mulliken overlap populations (MOP) for the same atom types. The latter are listed in Table 3 for different types of neighboring pairs of atoms in $Lu_7Ni_2Te_2$. In general, the pairwise MOP values increase as atoms separations decrease, but the shorter Lu−Lu separations do not always exhibit larger overlap populations, e.g., in the Lu_c-Lu_b vs Lu_b-Lu_b. The overall Lu metallic network has 3D character, the average MOP for interlayer bonding via Lu4 being ∼93% of that of intralayer ones.

There is naturally no indication of appreciable Te···Te or Ni···Ni bonding as they are not near neighbors. The metal layers normal to $\vec{b}$ are interlinked mainly by Lu−Te and Lu−Lu4 interactions. The number of heteroatom neighbors, the average Lu−Lu distances, and the average Lu−Lu MOP values in their polyhedra are listed in Table 4 for each of the four crystallographically independent Lu atoms. The *average* MOP of the Lu−Lu bonds increases with a decrease

(34) Shannon, R. D. *Acta Crystallogr.* **1976**, *32A*, 751.
(35) Hulliger, F.; Hull, G. W. *Solid State Commun.* **1970**, *8*, 1379.
(36) Pearson, R. G. *Inorg. Chem.* **1988**, *27*, 736.

in the number of the Te or Ni neighbors, indicating again that the polarities of Lu−Te (and Lu−Ni) interactions drain electrons from the Lu−Lu metal network and weaken the Lu−Lu bonding. From Lu2 to Lu3, the *average* MOP increases 26% with two fewer Te neighbors about the latter. Of course, we have not accounted for, or even estimated, the presumably considerable contributions to total stability of the polar (Madelung) energy in the bonding of Te to the more positive metal frameworks.

At first thought, it seems that E_F might be adjustable through substitution of altervalent elements without changing the whole structure because the electron count of a metallic phase is, in principle, continuously variable and evidently not very critical. For example, from Ni to the workable Ru, there are 8 fewer valence electrons per cell and E_F falls ∼0.4 eV, and from Ni to Cd, there would be 8 e^- more per unit, the E_F would rise ∼0.4 eV, and the electrons would still fill mainly Lu−Lu bonding states, just a small number of slightly antibonding Lu−Z states also being occupied. So, at first thought it might seem possible that a variety of interstitial metals, including the electron-richer Cu, Ag, or Cd, might also stabilize the 7:2:2 (and other) phases electronically and the Te might be replaceable as well, e.g., by Sb or I. But the usual problem here at present is the highly unpredictable stability of *alternate* phases of known or unknown structure, i.e., for Ag or Rh or I in other salts or intermetallics. Of course, experiments give us a quick answer, but much new chemistry is always beyond our imagination.

Conclusion

The $Lu_7Z_2Te_2$ (Z = Ni, Pd, Ru) phases are isostructural with the lighter rare-earth-metal telluride $Er_7Ni_2Te_2$[13] and also appear to be metallic. The structure can be viewed as metal layers normal to [010] that are formed by condensation of late-transition-metal-centered tricapped trigonal prisms and are further interlinked by bridging Lu and Te to form a 3D network. The Te atoms play the role of spacers between the layers but also contribute to the bonding. Extended Hückel calculations show that Lu−Lu metallic bonding is spread out into three dimensions, and that the polar Lu−Te and Lu−Z heteroatomic bondings are optimized as far as electron count. The energetically lower-lying Te and Ni partially oxidize Lu metal, Te especially, and withdraw electron density from the Lu metallic network, thus diminishing Lu−Lu interactions somewhat.

Supporting Information Available: Additional crystallographic data for Lu_7Ni_2Te and all crystallographic data for $Lu_7Pd_2Te_2$. This material is available free of charge via the Internet at http://pubs.acs.org.

IC030261K